Thin Film Morphology of Block Copolymer Blends with Tunable Supramolecular Interactions for Lithographic Applications

ARTICLE *in* MACROMOLECULES · MARCH 2010

Impact Factor: 5.8 · DOI: 10.1021/ma902843q

9 AUTHORS, INCLUDING:

Kulandaivelu Sivanandan
SEEO
18 PUBLICATIONS **388** CITATIONS
SEE PROFILE

Michael Dimitriou
University of California, Santa Barbara
25 PUBLICATIONS **566** CITATIONS
SEE PROFILE

Glenn H Fredrickson
University of California, Santa Barbara
434 PUBLICATIONS **28,272** CITATIONS
SEE PROFILE

DOI: 10.1021/ma902843q

Macromolecules
ARTICLE

Thin Film Morphology of Block Copolymer Blends with Tunable Supramolecular Interactions for Lithographic Applications

Chuanbing Tang,*[,†,⊥] Su-mi Hur,[†,‡] Brian C. Stahl,[†,∥] Kulandaivelu Sivanandan,[†] Michael Dimitriou,[†,∥] Eric Pressly,[†,∥] Glenn H. Fredrickson,*[,†,‡,∥] Edward J. Kramer,*[,†,‡,∥] and Craig J. Hawker*[,†,§,∥]

[†]*Materials Research Laboratory,* [‡]*Department of Chemical Engineering,* [∥]*Department of Materials, and* [§]*Department of Chemistry and Biochemistry, University of California, Santa Barbara, California 93106.* [⊥]*Current Address: Department of Chemistry and Biochemistry, University of South Carolina, 631 Sumter Street, Columbia, SC 29208.*

Received December 24, 2009; Revised Manuscript Received February 19, 2010

ABSTRACT: A modular and hierarchical self-assembly strategy using block copolymer blends (AB/B'C) with tunable supramolecular interactions is reported. By combining supramolecular assembly of hydrogen-bonding units with controlled phase separation of diblock copolymers, highly ordered square arrays or hexagonal arrays of cylindrical domains were obtained for mixtures of poly(ethylene oxide)-*b*-poly(styrene-*r*-4-hydroxystyrene) (PEO-*b*-P(S-*r*-4HS)) and poly(styrene-*r*-4-vinylpyridine)-*b*-poly(methyl methacrylate) (P(S-*r*-4VP)-*b*-PMMA) diblock copolymers under solvent annealing with controlled high humidity. The fraction of the H-bonded phenolic and pyridyl units was shown to be critical for both the generation of long-range order and controlling the spatial arrangement of the cylindrical domains. Both low absolute numbers and a near-stoichiometric ratio of pyridyl-to-phenolic groups are needed to produce ordered square arrays with separated PEO and PMMA domains, whereas a low ratio of pyridyl-to-phenolic groups facilitated the formation of ordered hexagonal arrays with mixed PEO and PMMA domains. Self-consistent field theory simulations suggest that the effective Flory−Huggins parameters between the various blocks control the stability of the different packing structures in this system. The modularity and tunability of this supramolecular block copolymer blending approach is a unique and powerful strategy to fabricate diverse nanostructures for a variety of applications such as block copolymer lithography.

Introduction

Block copolymers are a class of self-assembling soft materials comprising at least two covalently linked polymer chains,[1−3] where thermodynamic immiscibility between these blocks gives rise to a rich array of ordered nanostructures with periodicity on the scale of 10−100 nm. Such length scales have produced interest in using these block copolymers for applications ranging from microelectronic devices, data storage systems, membranes, photonic crystals, and so on.[4−9] The simplest diblock copolymers typically self-assemble into body-centered cubic spheres, hexagonally packed cylinders, double-gyroid, and lamellae nanostructures. Which of these are stable is mostly dictated by three experimental parameters: the degree of polymerization (N), the volume fraction of the blocks (f), and the Flory−Huggins interaction parameter (χ).[10−13] The chemical nature of the block segments determines χ, which in turn describes the segment−segment interactions.

With more than three decades of experiments and theory aimed at understanding the thermodynamic behavior of AB diblock copolymers,[2,3,14,15] it is important to explore block copolymer systems that can yield new and interesting ordered morphologies.[2,3] For example, linear ABC triblock copolymers have received significant attention because of the existence of a wide range of morphologies, such as periodic arrays of core/shell spheres and cylinders, tetragonal lattices of cylinders, and novel bicontinuous and tricontinuous ordered mesophases.[2,16,17] The greater diversity in morphology afforded by ABC triblock copolymers is due to their three binary interaction parameters, two independent volume fractions, and three different block sequences,[2,16−25] as opposed to one binary interaction parameter, one volume fraction, and a single block sequence for traditional diblock copolymers. Furthermore, the novel morphologies present in ABC triblocks can enable a broader range of applications by utilizing the physical and chemical properties of the three distinct blocks. Unfortunately, the synthesis of linear ABC triblock copolymers with precisely controlled block lengths is difficult, and the range of repeat units is limited.

A second strategy to diversify the morphologies achievable with block copolymers is to synthesize more complex block copolymer architectures such as star block copolymers.[26−29] Whereas the synthesis may be challenging, the introduction of architectural parameters adds further issues in controlling thin film structure. A third strategy that overcomes these issues is to blend simple diblock copolymers or homopolymers to give, for example, AB/CD, AB/BC, or AB/C systems. This approach is attractive for combining physical properties and significantly broadening the processing window.[30−33] Synthetically, the preparation of linear diblock copolymers can be more accessible and controllable than triblock copolymers or 3-D macromolecular architectures. In turn, the main challenge with these blend systems is an overwhelming tendency to exhibit macrophase separation.[34−37]

Inspired by complex and hierarchical natural systems where nanostructures are formed through a combination of covalently

*Corresponding authors. E-mail: ghf@mrl.ucsb.edu (G.H.F.); edkramer@mrl.ucsb.edu (E.J.K.); hawker@mrl.ucsb.edu (C.J.H.); tang.c@chem.sc.edu (C.T.).

 Published on Web 03/01/2010

Scheme 1. Synthesis of Diblock Copolymers PEO-*b*-P(S-*r*-4HS) and P(S-*r*-4VP)-*b*-PMMA via Controlled/Living Radical Polymerizations

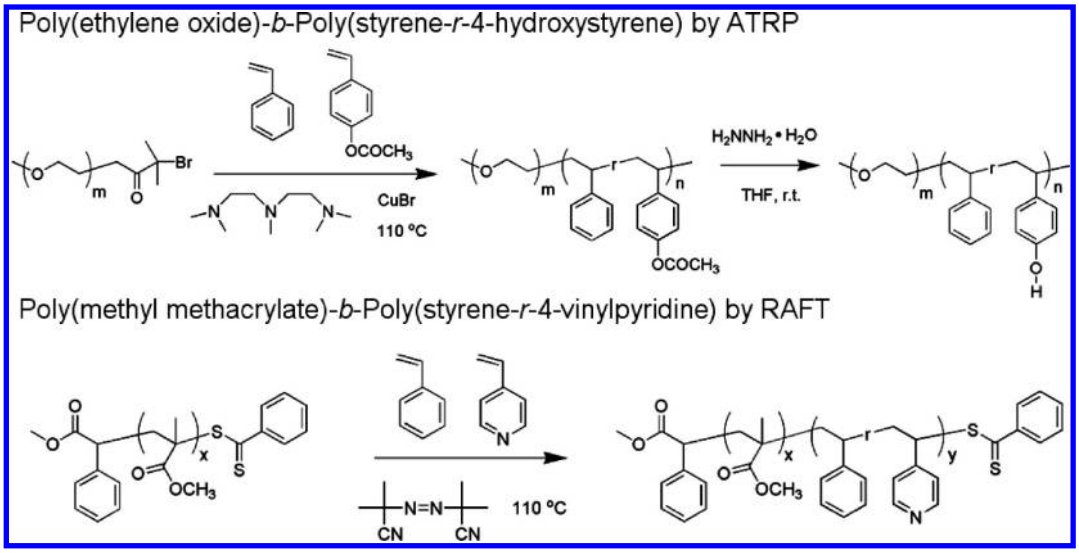

linked macromolecular subunits and noncovalent supramolecular interactions such as hydrogen bonding and ionic interactions, noncovalent interactions have been explored in the context of block copolymer blends.[38−43] The supramolecular interactions not only can prevent macrophase separation but also can provide a simple route to complex block copolymer morphologies that are difficult to achieve via a fully covalent synthesis route. Several approaches have been followed to obtain novel block copolymer structures by means of noncovalent intermolecular interactions. The first approach is to blend block copolymers with low-molecular-weight compounds that can form hydrogen bonds with one of the blocks.[44,45] The second approach is to blend block copolymers with a second polymer, either a homopolymer or a block copolymer, to produce AB/C,[46,47] AB/CD,[30,48] ABA/CD,[49] or ABC/AD blends,[31] where hydrogen bonding interactions can be formed between two different blocks so that complementary segments are mixed into one domain.

Motivated by elegant hierarchical structures reported in block copolymer blends with supramolecular interactions as well as the promise of various applications of their self-assembly in thin films,[6,50−74] we have recently introduced a modular and tunable supramolecular block copolymer, AB/B'C, blend system. In this case, attractive supramolecular (H-bonding) interactions occur between B and B' in addition to the nonspecific interactions present in the block copolymer alloy.[75] Unlike other previous reports in the literature, most of which utilized high concentrations of complementary H-bonding moieties (e.g., a pair of blocks or polymers with complementary H-bond donors and acceptors on every monomer unit),[30,31,46−49] the key to our design strategy is to use random copolymer blocks of B and B' containing a limited number of complementary hydrogen bonding units as comonomers so as to provide tunable attractions between the AB and B'C diblock copolymers. By controlling the level of incorporation of H-bonding units in B and B', the molecular weights and compositions of the block copolymers as well as the relative amounts of the two block copolymers in the alloy, square arrays of cylinders can be developed on silicon substrates and lithographically transferred with high fidelity, leading to highly ordered square arrays of cylindrical pores. In this article, we present detailed experimental results concerning the preparation of a library of block copolymer blends with tunable supramolecular interactions and report on their processing into thin films. We also compare the observed experimental morphologies with predictions obtained from numerical self-consistent field theory (SCFT). Particular attention is paid to the role of stoichiometry of the supramolecular bonding; experiments using B and B' blocks with different numbers of H-bonding units allow the role of stoichiometry and overall level of H-bonding groups on the domain morphology and order in the films to be studied. Finally, a possible mechanism underlying the formation of different morphologies is discussed.

Experimental Section

Synthesis of Poly(ethylene oxide)-*b*-poly(styrene-*r*-4-hydroxystyrene) (PEO-*b*-P(S-*r*-4HS)) and Poly(styrene-*r*-4-vinylpyridine)-*b*-poly(methyl methacrylate) (P(S-*r*-4VP)-*b*-PMMA) Diblock Copolymers. All diblock copolymers were synthesized, as described in our previous report (Scheme 1).[75] Synthesis of the diblock copolymers PEO-*b*-P(S-*r*-4HS) was achieved by atom transfer radical polymerization (ATRP) of styrene and 4-acetoxystyrene from a macroinitiator PEO-Br, followed by hydrolysis of the acetoxy groups using hydrazine. In select cases, diblock copolymers with a cleavable trityl ether linker between PEO and P(S-*r*-4HS) blocks were prepared by nitroxide-mediated polymerization using the same polymerization sequence.[76] Diblock copolymers P(S-*r*-4VP)-*b*-PMMA were synthesized by reversible addition−fragmentation chain transfer polymerization (RAFT)[76] in which a PMMA RAFT macroinitiator was chain extended with P(S-*r*-4VP). Monomer conversion analysis was carried out on chain extension using characteristic chemical shifts of ^{1}H NMR from CH_2=CH of monomers and CH_2−CH of polymers.

Preparation of Thin Films. Diblock copolymers PEO-*b*-P(S-*r*-4HS) and P(S-*r*-4VP)-*b*-PMMA were dissolved in either toluene or benzene solutions and blended in a 1:1 molar ratio. The mixtures were then spin coated onto a silicon substrate containing a 100 nm thick silicon oxide surface layer. We adjusted the film thickness, typically in the range of 40−70 nm, by controlling the solution concentration. The films were annealed up to 48 h under saturated toluene vapor supplied by a neighboring solvent reservoir in a sealed chamber that was placed in a homemade glovebox. The initial relative humidity in the sealed chamber was ∼40% (the ambient humidity in the lab). The humidity inside the glovebox was maintained at a relatively high humidity in the range of 82−95% by flowing moist air that was bubbled through a warm water reservoir. Once the solvent annealing time had elapsed, the chamber was quickly uncovered inside the glovebox, allowing both the evaporation of the organic solvent from the swollen film and the interaction between water vapor in the glovebox with the swollen film. Previous work already demonstrated that this controlled

Table 1. Number-Average Degree of Polymerization and Composition of AB and B'C Diblock Copolymers (the Last Digit of Each Sample Name Denotes the Average Number of H-bonding Units Per Chain)[a]

PEO-*b*-P(S-*r*-4HS)	$DP_{EO}/DP_S/DP_{4HS}$	f_{PEO} (wt %)	f_{PS} (wt %)	f_{P4HS} (wt %)
(**1a**) A-B_5*	113:150:**5**	23.0	71.9	2.8
(**1b**) A-B_7	113:147:**7**	23.8	72.4	3.8
(**1c**) A-B_12*	113:153:**12**	21.9	69.6	6.3
(**1d**) A-B_17	113:205:**17**	17.6	75.2	7.2
(**1e**) A-B_22	113:198:**22**	17.7	72.9	9.4
P(S-*r*-4VP)-*b*-PMMA	**$DP_{MMA}/DP_S/DP_{4VP}$**	**f_{PMMA} (wt %)**	**f_{PS} (wt %)**	**f_{P4VP} (wt %)**
(**2a**) B'-C_6	120:220:**6**	33.7	64.4	1.9
(**2b**) B'-C_8	120:195:**8**	36.3	61.3	2.4
(**2c**) B'-C_14	120:188:**14**	36.4	59.1	4.5
(**2d**) B'-C_15	90:173:**15**	31.5	63.0	5.5
(**2e**) B'-C_25	120:219:**25**	32.1	61.0	6.9
(**2f**) B'-C_36	120:252:**36**	28.6	62.4	9.0
(**2g**) B'-C_38	210:260:**38**	40.4	52.0	7.6

[a] DP is the degree of polymerization for each of the repeat units. * indicates diblock copolymers with a trityl ether linker between PEO and P(S-*r*-4HS) segments. All block copolymers have a polydispersity index below 1.25.

Scheme 2. Overall Structure and Graphical Representation of Diblock Copolymers Containing Tunable H-Bonding Donors or Acceptors: PEO-*b*-P(S-*r*-4HS) and P(S-*r*-4VP)-*b*-PMMA[a]

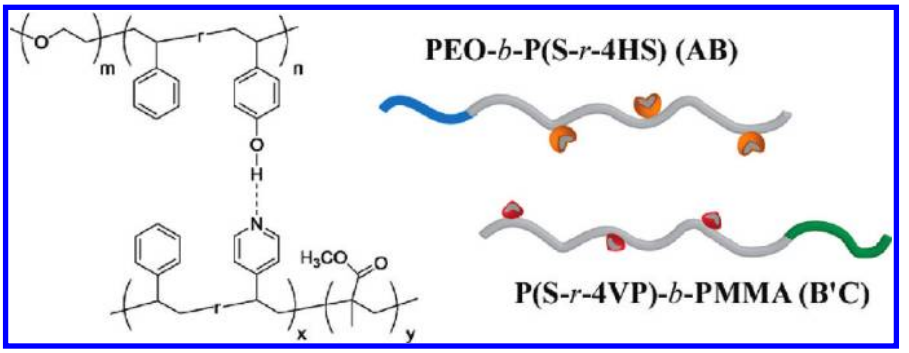

[a] Some of diblock copolymers PEO-*b*-P(S-*r*-4HS) have a cleavable trityl ether linker between PEO and P(S-*r*-4HS) segments.

humidity procedure induces lateral ordering of PEO domains on the surface.[24,25,77−80] After the solvent annealing process, some of the films were exposed to deep UV light (254 nm) at a dose of 25 J cm^{-2} (XX-15S, UVP, Inc.) under vacuum for 15−20 min to degrade the PMMA domains. Selected films with trityl-containing PEO-based block copolymers were further exposed to trifluoroacetic acid (TFA) vapor for 2 to 4 h, followed by methanol/water washing to remove the PEO domains.

Microscopy Imaging. Tapping mode scanning force microscopy experiments were carried out using a Multimode Nanoscope III system (Digital Instruments (now Veeco), Santa Barbara, CA). The measurements were performed using commercial Si cantilevers with a nominal spring constant and resonance frequency equal to 48 N/m and 190 kHz, respectively (ACL, Applied Nanostructures, Santa Clara, CA). Scanning electron microscopy (SEM) was carried out using a FEI XL30 Sirion FEG microscope operating at an acceleration voltage of 5 kV. The secondary electron image was collected in ultra-high-resolution mode at a working distance of ~5 mm. In addition, transmission electron microscopy (TEM) was used to image these block copolymer thin films. Block copolymer blend films on silicon wafers covered by a 100 nm thick layer of silicon oxide were immersed in a 10 wt % HF solution and transferred to a water bath, floated off the substrate, and placed on a Cu grid. TEM imaging of these was carried out using an FEI Tecnai G20 TEM operating at 200 kV.

Results and Discussion

The synthesis of well-defined diblock copolymers PEO-*b*-P(S-*r*-4HS) (denoted as AB) and P(S-*r*-4VP)-*b*-PMMA (denoted as B'C) with precisely controlled compositions was accomplished by atom transfer radical polymerization (ATRP) and reversible addition−fragmentation transfer polymerization (RAFT), respectively.[81−84] Table 1 lists the molecular weight characteristics for the library of AB (**1**) and B'C (**2**) diblock copolymers. This high degree of structural control allows the supramolecular interactions between the components of the blends to be tuned by changing the number of H-bonding donors or acceptors per block copolymer chain, as illustrated in Scheme 2. From the free radical copolymerization reactivity ratios of styrene and 4-acetoxystyrene (4AS),[85] our synthesis should produce almost ideal random copolymer blocks of P(S-*r*-4AS) when the conversion is kept low as for the PEO-*b*-P(S-*r*-4AS) synthesis. In contrast, the free radical copolymerization of styrene and 4-vinylpyridine does not produce "blocky" or ideal random copolymers but leads to alternating copolymers.[85] In the present case of diblock copolymers P(S-*r*-4VP)-*b*-PMMA, the number of 4VP units is small compared with the number of styrene units maintaining the distribution of 4VP units along the styrene backbone. Examination of the monomer conversion during preparation of these blocks confirmed these predictions based on the reactivity ratios. In select cases, the PEO-*b*-P(S-*r*-4AS) diblock copolymer contained a trityl linker between blocks; however, studies showed that this linker did not affect the overall morphology of the blends or parent diblock copolymer.[76,86,87]

To understand the phase behavior and structure/property relationships for these AB/B'C materials, diblock copolymers PEO-*b*-P(S-*r*-4HS) (AB) with a small number of H-bonding donor units per chain (i.e., 5 in **1a** and 7 in **1b**) were mixed with

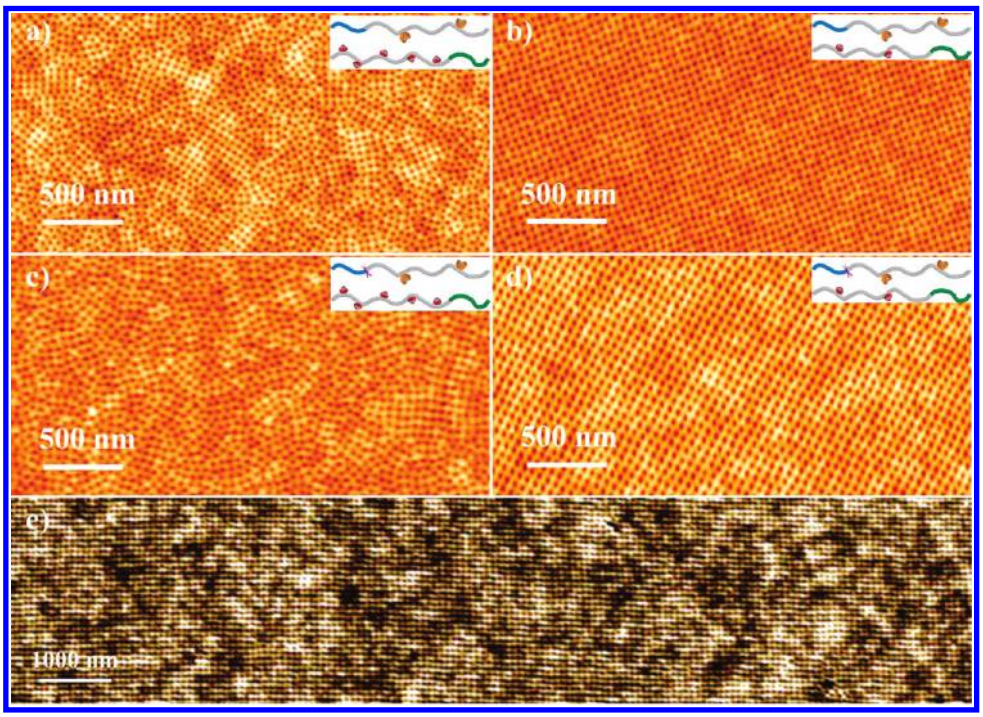

Figure 1. SFM height images of solvent annealed films of supramolecular block copolymer blends: (a) **1b**/**2c**; (b) **1b**/**2b**; (c) **1a**/**2c**; (d) **1a**/**2b**; and (e) **1a**/**2b**. SFM height image e shows a square array with grain size $>8\ \mu$m. Insets in each subfigure illustrate relative numbers of donors and acceptors. The pink $\times$ symbols represent trityl linkers. All of the following Figures use similar illustrations.

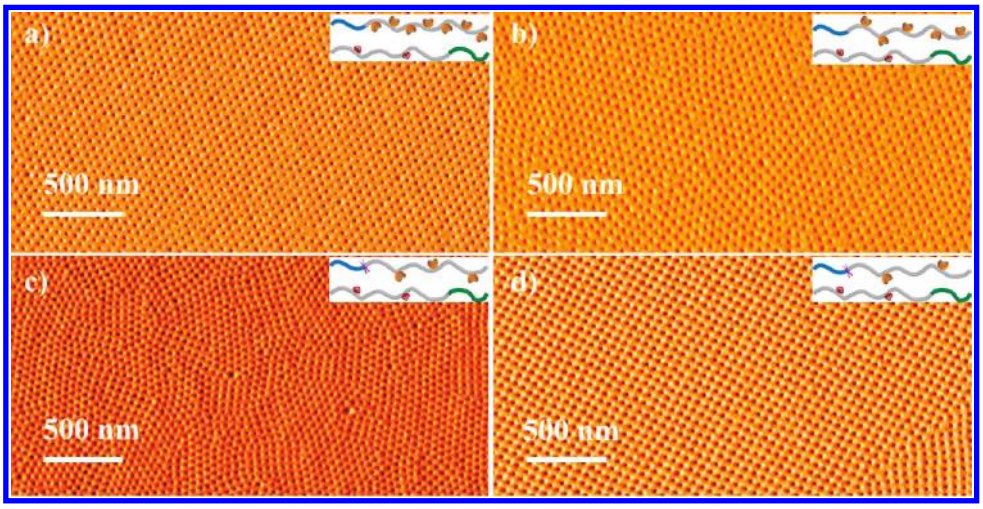

Figure 2. SFM phase images of solvent annealed films from supramolecular block copolymer blends: (a) **1e**/**2a**, (b) **1d**/**2a**, (c) **1c**/**2a**, and (d) **1a**/**2a**.

a series of diblock copolymers P(S-*r*-4VP)-*b*-PMMA (B'C) containing varying numbers of H-bonding acceptors in toluene. The blends were spun-cast onto silicon wafers, followed by solvent annealing in a controlled humidity environment under saturated toluene vapor. Figure 1 shows the SFM images of solvent annealed thin films of different blends. When the ratio of pyridyl-to-phenolic groups was larger than 2, these blends (**1a** and **2c**; **1b** and **2c**) produced arrays of disordered perpendicular cylinders, although some small grains of square arrays were observed (Figure 1a,c). When the ratio of pyridyl-to-phenolic groups was <1.5 (blends: **1a** and **2b**; **1b** and **2b**), square arrays with excellent in-plane ordering were formed (Figure 1b,d). Figure 1e shows an ordered square array with a grain size of $\sim10\ \mu$m, the largest obtained in this series of blends. However, if the PEO-*b*-P(S-*r*-4HS) copolymers had a significantly larger number of donor units per chain, as will be discussed further below, even ratios of pyridyl-to-phenolic groups <1.5 did not produce highly ordered square arrays. This result indicates that both the total number of phenolic group donors per chain and the ratio of pyridyl-to-phenolic groups are of critical importance if well-ordered square arrays are desired.

The effect of the number of donors per chains on the packing structures of blends was then investigated using a range of different blends. Initially, diblock copolymers B'C with ~6 pyridyl acceptors per chain were mixed with AB diblock copolymers containing varying numbers of phenolic donors per chain. When AB diblock copolymers with the highest number of donors per chain and therefore lowest ratio of pyridyl-to-phenolic groups (~0.27) were employed for the blend (**1e** and **2a**), highly ordered hexagonal arrays of vertical cylinders were observed in the thin films (Figure 2a). On increasing the ratio of pyridyl-to-phenolic groups to 0.36, the films of blends (**1d** and **2a**) still produced ordered hexagonal arrays of vertical cylinders (Figure 2b).

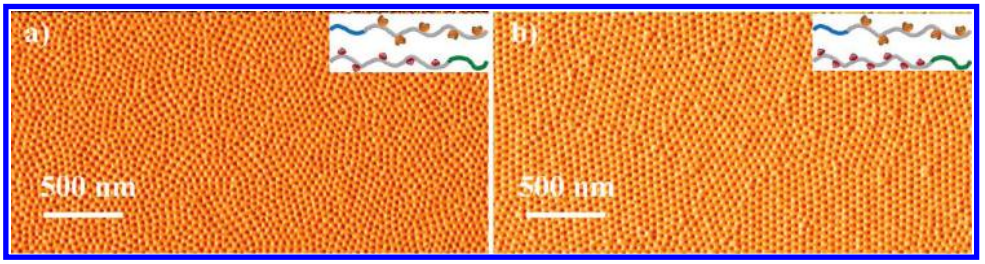

Figure 3. SFM phase images of solvent annealed films from supramolecular block copolymer blends: (a) **1e**/**2e** and (b) **1e**/**2f**.

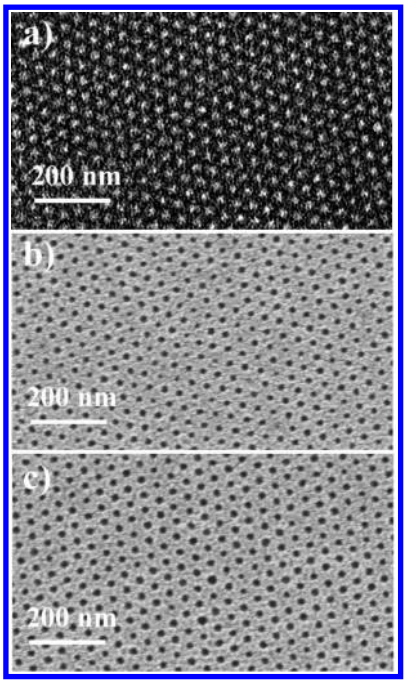

Figure 4. TEM and SEM images of solvent annealed films of supramolecular block copolymer blends (**1c/2d**): (a) UV irradiated, (b) TFA exposed, and (c) TFA exposed and then UV irradiated.

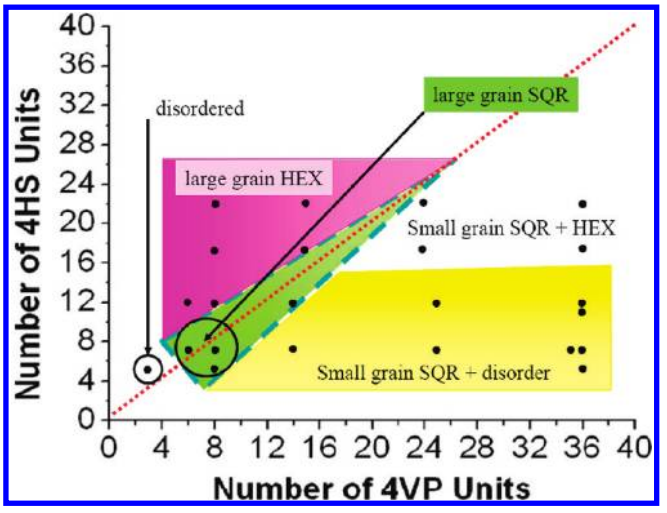

Figure 5. Morphology of solvent annealed films from supramolecular block copolymer blends as a function of number of H-bonding component units per chain. In general, the extent of the grains of SQR decreases as the number of H-bonding groups increases along the diagonal of the SQR region. Points at or close to the boundary between the SQR and HEX regions show coexistence of SQR and HEX arrays.

Coexistence of hexagonal and square arrays was observed for blends (**1c** and **2a**) with a ratio of pyridyl-to-phenolic groups of 0.5 (Figure 2c). When the ratio of pyridyl-to-phenolic groups was further increased to 1.2, the morphology of the blend (**1a** and **2a**) was again observed to be ordered square arrays (Figure 2d).

In direct contrast, blends of block copolymers with larger numbers of both donor and acceptor H-bonding units per chain were observed to have significantly different morphological behavior by SFM. Figure 3 shows two thin film blends containing a block copolymer with the largest number of H-bonding donors per chain (ca. 22) and with two block copolymers with large numbers of H-bonding acceptors (ca. 25 and 36). For the blend (**1e** and **2e**) with a ratio of pyridyl-to-phenolic groups of 1.14, coexistence between small grains of square and hexagonal arrays (Figure 3a) was observed, whereas the blend (**1e** and **2f**) with a ratio of pyridyl-to-phenolic groups of 1.64 showed small hexagonal grains (Figure 3b).

The inconsistent appearance of hexagonal arrays, in some cases at ratios R of pyridyl-to-phenolic groups exceeding 1.5 and in other cases at values of $R < 1.2$, prompted us to explore the locations of PEO and PMMA domains using TEM and SEM. The TEM images (Figure 4a) indicate that the UV-irradiated film (in this case with $R = 1.25$, **1c** and **2d**) shows ordered hexagonal structures with a single set of brighter domains. In this case, the contrast of the brighter domains is more diffuse when compared with the UV-irradiated PMMA domains of the ordered square array structure. The absence of a second set of cylindrical domains with a different contrast from the first strongly suggests that the cylinder domains seen in the hexagonal phase of the **1c** and **2d** blend consist of a mixture of PEO and PMMA blocks. To confirm further that PEO and PMMA blocks are mixed, films of a blend consisting of **1c** with a trityl-linked PEO block and **2d** were characterized using SEM. The films were treated with TFA, followed by UV irradiation to remove sequentially PEO domains and PMMA domains, respectively. Initial films after TFA treatment revealed ordered hexagonal packed nanopores with a periodicity of 36 nm in the matrix of polystyrene (Figure 4b), whereas films after both TFA and UV treatment show hexagonal packed nanopores with a periodicity of 35 nm (Figure 4c), which is very similar to TFA-treated films. Films that were subjected to UV irradiation, followed by TFA treatment, also displayed similar packing structures and lattice parameters, demonstrating that the PEO and PMMA block chains are mixed in the hexagonally ordered cylindrical domains.

In total, the domain morphologies of two dozen equimolar AB and B'C supramolecular block copolymer blend films with different numbers of donor and acceptor H-bonding units were investigated using SFM, SEM, and TEM. Figure 5 shows graphically the results as a function of the numbers of H-bonding donor and acceptor units per block. This plot shows three distinct morphological trends in these supramolecular block copolymer blends. When the number of pyridyl groups per B' random block is much larger than the average number of phenolic groups in each B random block, the films exhibited poor ordering with

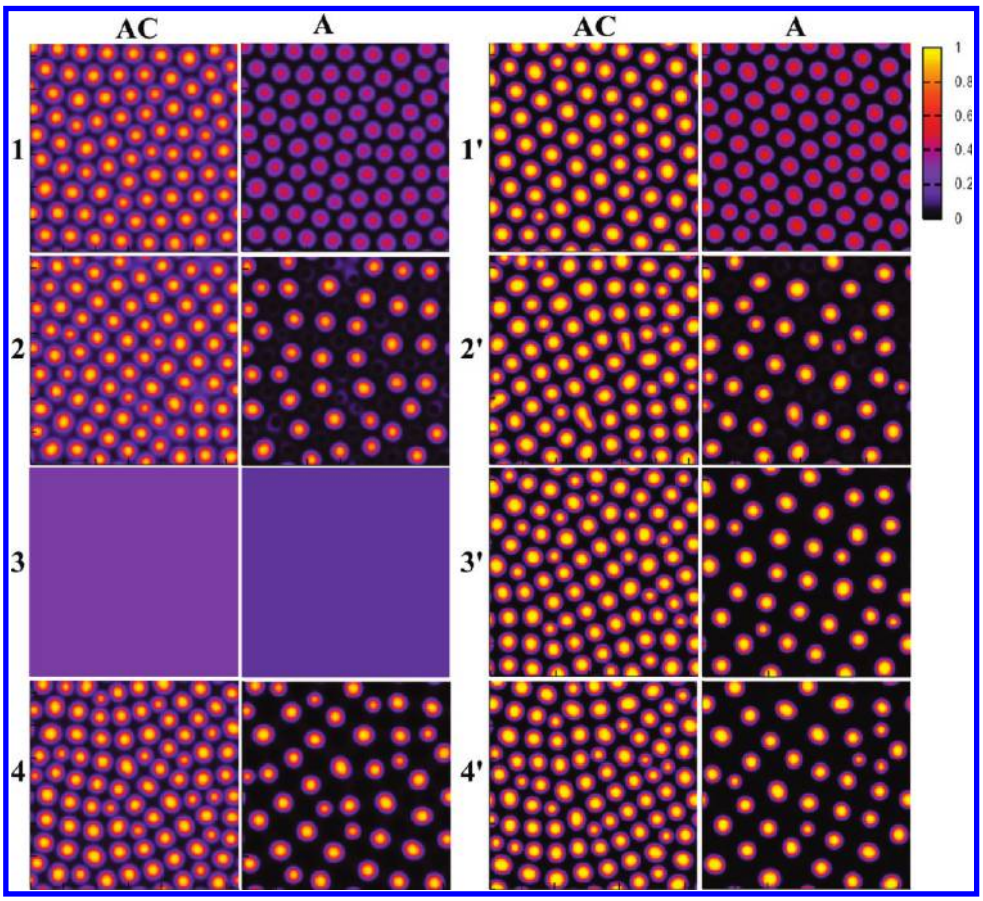

Figure 6. Representative minor block (A and C) segment density plots from SCFT simulations for various χ(AC)N, constant $\chi N = 18.875$, and χ(BB')$N = -7.468$ (1, 2, 3, and 4) or $\chi N = 25$ (1′, 2′, 3′, and 4′). Rows correspond to different values of χ(AC)N: (1, 1′) χ(AC)$N = 10$; (2, 2′) χ(AC)$N = 20$; (3, 3′) χ(AC)$N = 30$; (4, 4′) χ(AC)$N = 40$. The sum of the A and C segment densities is shown in the AC columns, whereas the A segment density is shown in the A column. Each subfigure is denoted in the text as "Figure 6-*rc*", where *r* is the row number and *c* is the column number of the particular plot in the graphics array.

small grains of square arrays, hexagonal arrays, or both. When the number of phenolic groups per B block was much more than the number of pyridyl groups per B' block, ordered hexagonal arrays were the dominant morphology observed. Square arrays were obtained in films of blends containing a ratio of pyridyl-to-phenolic groups < 1.5, regardless of the absolute numbers of H-bonding components. However, highly ordered square arrays were achieved only when the ratio of pyridyl-to-phenolic groups was < 1.5 and when both B and B' blocks had small numbers of H-bonding components. If the number of H-bonding units in the B and B' units was further reduced, the blend films become completely disordered, with some macrophase-separated domains in evidence.

To gain further insight into the role of supramolecular interactions on the microdomain ordering, we conducted a series of SCFT simulations.[88,89] In particular, we examined a model AB/B'C diblock copolymer blend in which the supramolecular interactions are crudely accounted for by a nonspecific contact attraction between B and B' segments (χ(BB') < 0), as in our previous study.[75] Of course, hydrogen bonding is a specific supramolecular interaction that involves functional groups at localized sites that saturate upon bonding, so a more sophisticated association model should be employed for a comprehensive study.[90] Nonetheless, a simple SCFT model utilizing effective χ parameters proves sufficient to understand qualitatively aspects of the self-assembly of our AB/B'C blend system and its dependence on the relative strength of the interactions between segments.

In the simulations, the lengths of the AB and B'C diblock copolymers were set equal, and the length of each minor block (A or C) was set equal to 30% of its respective block copolymer chain length. For the results of the simulations displayed in Figure 7, the interaction parameters were set to be χ (BB')$N = -7.468$ and χ(AB)$N = \chi$(AB')$N = \chi$(BC)$N = \chi$(B'C)$N = \chi N = 18.875$ for one series and 25 for another. The only independent parameter remaining is χ(AC)N, which was set equal to 10, 20, 30, and 40 for a second series of simulations. A negative value of χ(BB')N corresponds to attractive interactions between the major blocks B and B'. Large-cell 2-D SCFT simulations with periodic boundary conditions (cell size $30R_g$ by $30R_g$) of this model were launched from random initial fields. Even though many defects were observed, ordered structures could be identified in the simulated morphologies. In both series shown in Figure 6, the AC columns show the sum of the density of the A and C segments, whereas the A columns show the density of just the A component for different values of the interaction parameter, χ(AC)N. For the smallest value of χ(AC)N (χ(AC)$N = 10$), the minor blocks (A and C) intermix to form hexagonally arranged cylinders surrounded by a corona composed of B and B' (Figure 6-1AC, -1A, -1′AC, and -1′A). However, as χ(AC)N is increased to 20, a transition occurs. The A and C segments segregate into cylinders that are predominantly either A or C to reduce the increasingly unfavorable A/C contacts, but a small volume fraction of A remains mixed into the shell of the C cylinders and vice versa (Figure 6-2AC, -2A, -2′AC, and -2′A). The A cylinders are packed tetragonally to distribute more uniformly around the C cylinders and vice versa. Increasing χ(AC)N to 25 seems to reduce slightly the amount of A mixed in the shell of C cylinders. As χ(AC)N is increased to

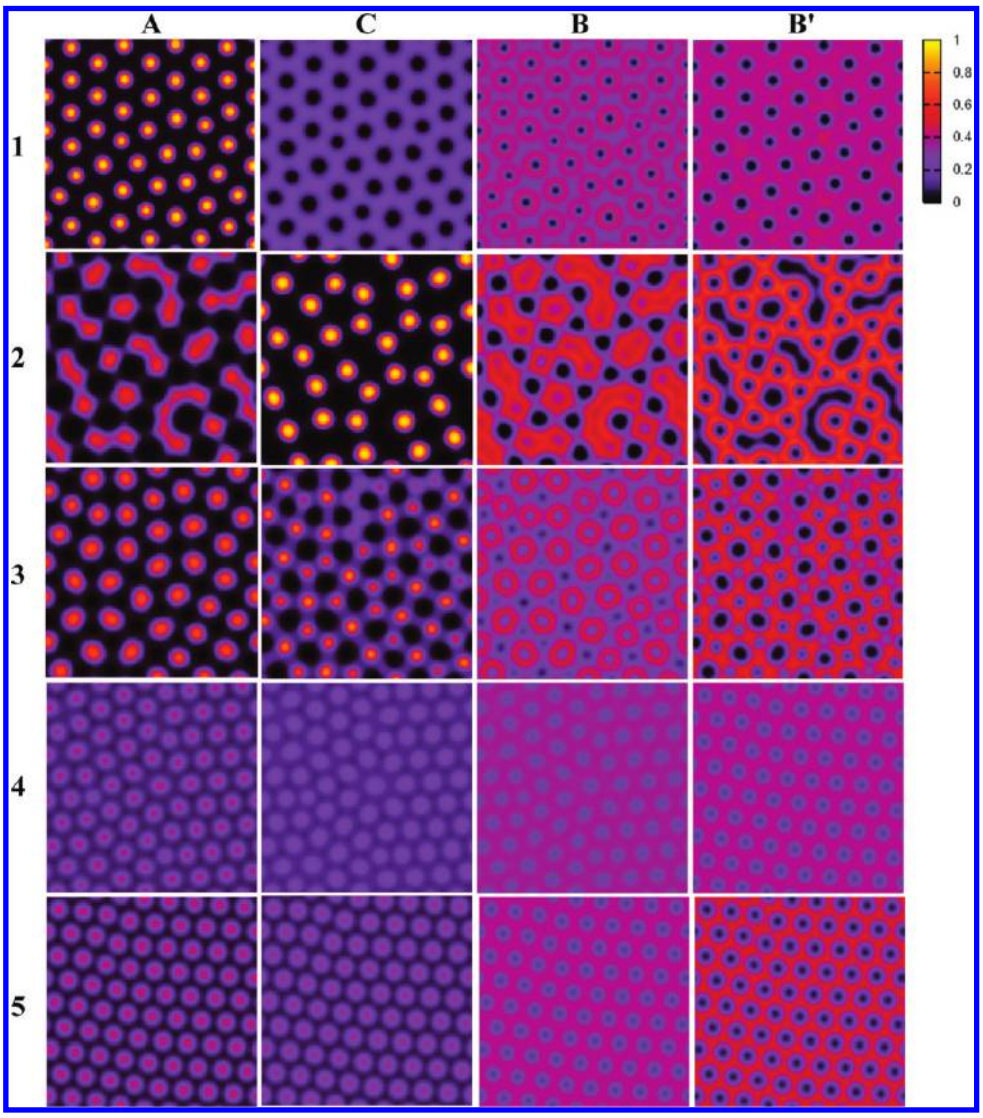

Figure 7. Possible microdomain orderings with different sets of interaction parameters of (1) χN(BC) = 5, (2) χN(AB) = 5, (3) χN(AB) = χN(BC) = 5, (4) χN(AB) = χN(BC) = χN(AC) = 10, and (5) χN(AB) = χN(BC) = 10, χN(AC) = 5. In each row, all of the other χN remained the same (χN = 18.875, χ(AC)N = 40, and χ(BB')N = −7.468) if not listed. Each subfigure is denoted in the text by "Figure 7-*rc*", where *r* is the row number and *c* the column number of the particular plot in the graphics array.

30 for χN = 18.875, the free energy cost for A/C contacts is larger than that for A/B(B') and C/B(B') contacts. Rather than further diminish the amount of intermixing between the A and C cylinders, which apparently carries a high chain stretching cost, the system instead transforms into a disordered state (Figure 6-3AC and -3A). However, upon increasing χN to 25, the system does not exhibit a disordered state, as shown in Figure 6-3′AC and -3′A. In this case, and with χ(AC)N = 30, the cylinders become pure A or pure C, and essentially no intermixing is observed. As χ(AC)N is further increased to 40, this situation is maintained, and cylinders composed solely of either the A or C components are formed in the matrix of B and B' (Figure 6-4AC, -4A, -4′AC, and -4′A). Because there is no A/C interface, the free energy is independent of χ(AC)N. The tetragonal lattice allows for a more uniform distribution of A and C cylinders relative to each other.

To gain insight into why hexagonal arrays were formed in experiments when phenolic groups in the B block were in large excess compared with pyridyl groups in the B' block, we conducted SCFT simulations in which the effective interaction parameters χ(AB) and χ(BC) were individually or collectively reduced relative to the others. The rationale is that an excess of phenolic groups in relation to pyridyl groups leaves residual phenols on the B blocks that can hydrogen bond to either PEO segments (A blocks) or PMMA segments (C blocks). This would serve to lower the values of χ(AB) and χ(BC).

Figure 7 shows the results of such simulations with representative density plots of each component. In Figure 7-1, χ(BC)N is decreased to 5 while maintaining the other parameters (χ(AB)N = χ(AB')N = χ(B'C)N = χN = 18.875) and with fixed χ(AC)N = 40. In contrast with the tetragonal arrays observed in Figure 6-4 and -4′, in Figure 7-1A we observe hexagonal arrays of A cylinders with the C blocks mixed into the continuous B/B' domain. If the C block was also to form separated cylinders, then the B chains attached to the A cylinders would have to stretch strongly to make contact with C, and such an arrangement would thus not be stable. The lower free energy penalty for BC contacts encourages C to mix with B, even though there remains a significant penalty for mixing B' and C. However, a small χ(BC) and the negative χ(BB') compensates for the penalty of mixing B' and C, and the B, B', and C mixing also lead to a reduced stretching of the B and B' blocks resulting from the close-packed hexagonal structure. The domain spacing in Figure 7-1 is larger than the spacing in hexagonal arrays with A

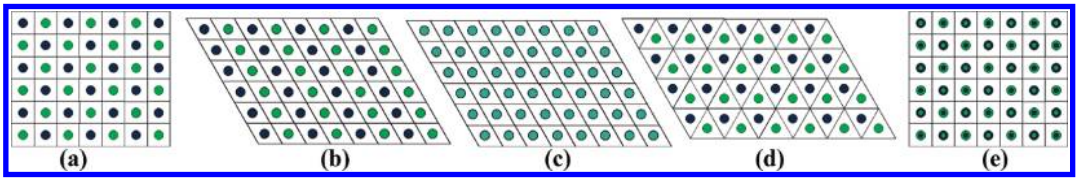

Figure 8. Possible packing structures from symmetric linear ABC triblock copolymers to form cylindrical patterns: (a) tetragonal packing with C_4 symmetry; (b) hexagonal packing (A and C are separated and must have same domain size); (c) hexagonal packing with C_6 symmetry (A and C mixed); (d) hexagonal packing with C_3 symmetry (both A and C have three-fold axis); and (e) tetragonal packing with C_4 symmetry. A and C domains have different colors. Another color used for mixed A and C.

and C mixed cylinders (Figure 6-1 and -1′) because of the larger volume fraction of polymer blocks (B, B', and C rather than just B and B') making up the matrix.

In Figure 7-2, χ(AB) is decreased to 5, whereas all other parameters are maintained the same. As A and B segments become more miscible, the domains of A become more dispersed, irregular, and larger. Unlike the results in Figure 7-1, smaller χ(AB) increases the tendency to macrophase separate, as shown in the Figure 7-2A because A and B are bound together in the same block copolymer. One can think of adding such a poorly segregated block copolymer as similar to adding a homopolymer with marginal miscibility (because of the strong repulsion between A and B'). When χ(AB) and χ(BC) are simultaneously decreased, a poorly ordered tetragonal phase was observed (Figure 7-3). In this case, B has same interaction strength with A and C. Whereas B tries to mix with C by pulling C into the matrix, B segments also partially mix with A by forming core−shell cylinders with predominantly A in the core and more B in the shell. As a consequence, a smaller volume fraction of B is mixed in the matrix compared with the case shown in Figure 7-1. Therefore, the enthalpy advantage from B/C contacts by pulling C into the matrix is decreased, and this smaller advantage is not enough to compensate for the penalty of mixing B' and C. The system therefore prefers a tetragonal structure, where C and mixed A/B cylinders form staggered square lattices. The diameter of the A/B mixed cylinders is larger than that of the C cylinders.

We also conducted a series of SCFT simulations to investigate the role of χ(AC)N on the morphology of AB/B'C blends. In part, this was motivated by the complex nature of the PEO-PMMA interaction throughout our film processing steps. PEO and PMMA are known to be miscible under dry conditions in the melt. However, during solvent annealing conditions under high humidity that we employ, hydrated PEO (A) blocks are apparently sufficiently incompatible with PMMA (C) blocks to form separate domains with tetragonal order, an observation already made in our previous study.[75] Nonetheless, because the water content of the film can vary significantly during and after the solvent annealing step, the effective PEO-PMMA interaction embodied by χ(AC)N is presumably highly time- and process-dependent and is therefore subject to considerable uncertainty. Figure 7-4 shows the effect of decreasing χ(AC)N in concert with decreasing χ(AB)N and χ(BC)N. In this example χ(AC)N, χ(AB)N, and χ(BC)N are set to 10, whereas χ(BB')N, χ(AB')N, and χ(B'C)N remain same. Similar to the situation shown in Figure 6, a small value of χ(AC)N encourages A/C mixing, thus forming hexagonally packed A/C mixed cylinders but with weaker segregation relative to the matrix B and B' blocks. In Figure 7-5, χ(AC)N is further decreased to 5, whereas χ(AB)N and χ(BC)N remain fixed at 10. Figure 7-5 shows that this further decrease in χ(AC) increases the segregation of A and C in the cylinders by favoring A/C mixing, thus excluding B and B' from the A/C mixed cylinder domains.

Tetragonal lattices in the bulk state of block copolymers were experimentally observed in a symmetrical linear ABC triblock copolymer by Mogi et al,[16,17] thus prompting us to compare the supramolecular block copolymer blends AB/B'C with the linear ABC counterparts. In the Mogi et al. system of polyisoprene-*b*-polystyrene-*b*-poly(2-vinylpyridine) (PI-*b*-PS-*b*-P2VP), the Flory−Huggins interaction parameter between PI and P2VP is larger than the other two interaction parameters (χ(PI-P2VP) > χ(PI-PS) ≈ χ(PS-P2VP)). PI and P2VP, each about 12−18% by volume of the block copolymer, assemble to produce two kinds of cylindrical domains of end-block segments, with a tetragonal pattern. However, no hexagonal packing was observed for these triblock copolymers in the bulk. Matsen[20] used SCFT to map the morphology of symmetrical linear ABC triblock copolymers as a function of χ(AC)/χ (χ = χ(AB) = χ(BC)). When χ(AC)/χ = 1, the cylinders form tetragonal lattices with C_4 symmetry that facilitates a relatively uniform distribution of A and C domains despite the fact that this lattice is not a close packed structure, as shown schematically in Figure 8a. In contrast, the formation of the structure shown in Figure 8b requires an asymmetric distribution of bridging chains of the midblock B matrix if separate A and C cylinder domains form, and this structure is not observed in the SCFT results of Matsen. When χ(AC)/χ is decreased below a certain value, the A and C end blocks mix, leading to a stable hexagonal phase with C_6 symmetry that is similar to the hexagonal phase in diblock copolymers (Figure 8c). Another possibility is that both A and C can form separate hexagonal structures with independent C_6 symmetry. These structures in total actually have a three-fold axis, and its point symmetry is C_3, as shown in Figure 8d. Note that the vertices of the triangles cannot be occupied by cylinders in a C_3 planar structure. Putting a cylinder of either color at the vertex leads to frustration, but the fact that each A cylinder has only three nearest neighbor C cylinders rather than four in the tetragonal structure means that some of the bridging B block chains must stretch more to fill the vertex than to fill the four-fold vertex in the tetragonal structure. This excess stretching presumably accounts for why the morphology in Figure 8d is not seen either in the theoretical work of Matsen or in the experiments of Mogi and coworkers.[16,17,20]

In the present article and in our previous work,[75] we simulated supramolecular AB/B'C block copolymer blends using a model and SCFT approach similar to Matsen. With χ(AC)N = 55 > χN = χ(AB)N = χ(B'C)N = χ(AB')N = χ(BC)N = 14 and χ(BB')N = −3.5, our simulations revealed that square-packed cylinders in the AB/B'C system have a lower free energy density than AC mixed hexagonally packed cylinders, which is the stable phase in simple AB diblock copolymers. Although in the supramolecular blend system, the A and C blocks are covalently linked to different chains, attractive interactions between B and B' blocks cause the blend to self-assemble in a similar fashion to symmetric linear ABC triblock copolymers. Presumably, this is because the favorable B−B' segmental mixing can occur at relatively uniform B and B' block extensions, and the reversible nature of the hydrogen bonds can facilitate bond rearrangements to relax any residual stresses in the B/B' domain. However, the rationale for the formation of hexagonal structures in a range of these blend films is an open question. If PEO and PMMA domains are not intermixed and each have separate hexagonal symmetry, the surface morphology of these PEO and PMMA domains would appear like the structure shown in Figure 8d.

However, such packings were not observed experimentally. Other structures, such as that shown in Figure 8b, were also not detected by SFM, TEM, or SEM. Instead, TEM and SEM demonstrated the formation of hexagonal structures with PEO and PMMA mixed, similar to the structure in Figure 8c. Because Matsen showed that for symmetric ABC triblocks, the formation of the structure in Figure 8c can be driven by a decrease in χ(AC), we were motivated to perform similar SCFT simulations for the AB/B'C system, exploring not only the role of A−C but also the role of A−B, B−C, and B−B' interactions. As described above, χ(AC) in the AB/B'C system indeed plays a critical role in the formation of different packing structures. When the repulsion between A and C is small, each cylinder is composed of mixed A and C blocks, and the cylinders pack hexagonally with C_6 symmetry similar to simple diblock copolymers (Figure 8d). However, for increased χ(AC), the cylinders are substantially composed of either the A or C component to avoid A/C contacts. The A cylinders are packed in a tetragonal lattice with C_4 symmetry to distribute uniformly around the C cylinders and vice versa.

The transition between hexagonal and tetragonal structures driven by increasing χ(AC) involves a structural rearrangement of cylinders. Therefore, the intermediate between the two structures is likely a tetragonal morphology consisting of C cylinders with small amounts of A dissolved in the shell and of A cylinders with small amounts of C dissolved in the shell, as illustrated in Figure 8e. Such intermediate structures have indeed been revealed by our SCFT simulations for the supramolecular AB/B'C alloy. It is possible that a similar minor amount of AC mixing exists in the tetragonal phase of the symmetric linear ABC triblock copolymers near the transition from hexagonal to tetragonal (corresponding to ABC chains looping back into the same domain), but Matsen did not report such mixing.[20]

Still puzzling is why separate PEO and PMMA domains form for some of the blends but not others, especially given that great effort was taken to ensure that the processing conditions (including humidity) were not altered and the chemical variations were restricted to the B and B' blocks. The fact that mixed PEO/PMMA domains with hexagonal packing were observed primarily in cases with an excess of H-bonding donors suggests that "unintentional" H-bonds between 4HS and MMA and/or 4HS and EO are to be implicated. Our SCFT studies have revealed that hexagonal phases can be formed by lowering χ(AB), χ(BC), or both, as would be the expected influence of such unintentional bonds, but unfortunately, these do not correspond to the hexagonal phase with mixed A/C cylinders.

Overall, whereas our SCFT simulations do not provide a definitive explanation for the observed morphology trends with donor−acceptor stoichiometry, they are revealing in terms of the role that the various binary interactions play in dictating hexagonal versus tetragonal packing in AB/B'C alloys.

Conclusions

A modular and hierarchical self-assembly strategy for the generation of highly ordered square and hexagonal arrays based on the blending of diblock copolymers (AB/B'C) with tunable supramolecular interactions (H-bonding) has been developed. By combining supramolecular assembly of H-bonding phenolic and pyridyl units with controlled microphase separation of well-defined diblock copolymers, it was shown that control over the number of complementary donor and receptor H-bonding groups is critical for achieving good order as well as controlling the local packing of cylindrical domains. The production of ordered square arrays is favored at low levels of H-bonding units incorporated per chain as well as near stoichiometric ratios of complementary H-bonding donors and acceptors. Hexagonal packings with mixed A and C domains were observed when the number of H-bond donors per chain is greater than the number of acceptors. SCFT simulations suggest a critical role for the interaction parameter χ(AC) in distinguishing square and hexagonal packings. Unfortunately, this parameter is not well-defined for the present system under the humidity controlled solvent annealing conditions employed, nor is it useful in explaining tetragonal to hexagonal transitions observed by changing donor−acceptor stoichiometry under otherwise identical process conditions. In conclusion, it is anticipated that this modular and tunable supramolecular block copolymer approach can be extended as a general strategy to prepare diverse nanoscale polymeric structures and assemblies based on a range of supramolecular interactions.

Acknowledgment. This work was supported by the Nanoelectronics Research Initiative under contract RID#1549 (SRC/NRI), the Focus Center Research Program (FCRP) − Center on Functional Engineered Nano Architectonics (FENA), and the National Science Foundation under the MRSEC program (UCSB MRL, DMR-0520415). B.C.S. gratefully acknowledges support of a Bonderson Fellowship.

References and Notes

(1) Bates, F. S.; Fredrickson, G. H. *Annu. Rev. Phys. Chem.* **1990**, *41*, 525–557.
(2) Bates, F. S.; Fredrickson, G. H. *Phys. Today* **1999**, *52*, 32–38.
(3) Fredrickson, G. H.; Bates, F. S. *Annu. Rev. Mater. Sci.* **1996**, *26*, 501–550.
(4) Hadjichristidis, N.; Pispas, S.; Floudas, G. *Block Copolymers: Synthetic Strategies, Physical Properties, and Applications*; John Wiley & Sons, Inc.: Hoboken, NJ, 2003.
(5) Lazzari, M.; Liu, G.; Lecommandoux, S. *Block Copolymers in Nanoscience*; Wiley-VCH: Weinheim, Germany, 2007.
(6) Bang, J.; Jeong, U.; Ryu, D. Y.; Russell, T. P.; Hawker, C. *J. Adv. Mater.* **2009**, *21*, 4769–4792.
(7) Ross, C. *Annu. Rev. Mater. Res.* **2001**, *31*, 203–235.
(8) Hamley, I. W. *The Physics of Block Copolymers*; Oxford University Press: Oxford, U.K., 1998.
(9) Park, C.; Yoon, J.; Thomas, E. L. *Polymer* **2003**, *44*, 6725–6760.
(10) Hajduk, D. A.; Harper, P. E.; Gruner, S. M.; Honeker, C. C.; Kim, G.; Thomas, E. L.; Fetters, L. J. *Macromolecules* **1994**, *27*, 4063.
(11) Helfand, E.; Wasserman, Z. R. *Macromolecules* **1978**, *11*, 960–966.
(12) Helfand, E.; Wasserman, Z. R. *Macromolecules* **1980**, *13*, 994–998.
(13) Matsushita, Y.; Mori, K.; Saguchi, R.; Nakao, Y.; Noda, I.; Nagasawa, M. *Macromolecules* **1990**, *23*, 4313–4316.
(14) Helfand, E. *Macromolecules* **1975**, *8*, 552–556.
(15) Leibler, L. *Macromolecules* **1980**, *13*, 1602–1617.
(16) Mogi, Y.; Kotsuji, H.; Kaneko, Y.; Mori, K.; Matsushita, Y.; Noda, I. *Macromolecules* **1992**, *25*, 5408–5411.
(17) Mogi, Y.; Nomura, M.; Kotsuji, H.; Ohnishi, K.; Matsushita, Y.; Noda, I. *Macromolecules* **1994**, *27*, 6755–6760.
(18) Nakazawa, H.; Ohta, T. *Macromolecules* **1993**, *26*, 5503–5511.
(19) Chen, H.-Y.; Fredrickson, G. H. *J. Chem. Phys.* **2002**, *116*, 1137–1146.
(20) Matsen, M. W. *J. Chem. Phys.* **1998**, *108*, 785–796.
(21) Bailey, T. S.; Pham, H. D.; Bates, F. S. *Macromolecules* **2001**, *34*, 6994–7008.
(22) Rzayev, J.; Hillmyer, M. A. *Macromolecules* **2005**, *38*, 3–5.
(23) Rzayev, J.; Hillmyer, M. A. *J. Am. Chem. Soc.* **2005**, *127*, 13373–13379.
(24) Bang, J.; Kim, S. H.; Drockenmuller, E.; Misner, M. J.; Russell, T. P.; Hawker, C. J. *J. Am. Chem. Soc.* **2006**, *128*, 7622–7629.
(25) Tang, C.; Bang, J.; Stein, G. E.; Fredrickson, G. H.; Hawker, C. J.; Kramer, E. J.; Sprung, M.; Wang, J. *Macromolecules* **2008**, *41*, 4328–4339.
(26) Hadjichristidis, N.; Iatrou, H.; Behal, S. K.; Chludzinski, J. J.; Disko, M. M.; Garner, R. T.; Liang, K. S.; Lohse, D. J.; Milner, S. T. *Macromolecules* **1993**, *26*, 5812–5815.
(27) Sioula, S.; Hadjichristidis, N.; Thomas, E. L. *Macromolecules* **1998**, *31*, 5272–5277.
(28) Huckstadt, H.; Gopfert, A.; Abetz, V. *Macromol. Chem. Phys.* **2000**, *201*, 296–307.

(29) Takano, A.; Wada, S.; Sato, S.; Araki, T.; Hirahara, K.; Kazama, T.; Kawahara, S.; Isono, Y.; Ohno, A.; Tanaka, N.; Matsushita, Y. *Macromolecules* **2004**, *37*, 9941–9946.
(30) Asari, T.; Matsuo, S.; Takano, A.; Matsushita, Y. *Macromolecules* **2005**, *38*, 8811–8815.
(31) Abetz, V.; Goldacker, T. *Macromol. Rapid Commun.* **2000**, *21*, 16–34.
(32) Vaidya, N. Y.; Han, C. D. *Macromolecules* **2000**, *33*, 3009–3018.
(33) Mao, H.; Arrechea, P. L.; Bailey, T. S.; Johnson, B. J. S.; Hillmyer, M. A. *Faraday Discuss.* **2005**, *128*, 149–162.
(34) Olmsted, P. D.; Hamley, I. W. *Europhys. Lett.* **1999**, *45*, 83–89.
(35) Frielinghaus, H.; Hermsdorf, N.; Sigel, R.; K., A.; Mortensen, K.; Hamley, I. W.; Messe, L.; Corvazier, L.; Ryan, A. J.; van Desschoten, D.; Wilhelm, M.; Floudas, G.; Fytas, G. *Macromolecules* **2001**, *34*, 4907–4916.
(36) Kimishima, K.; Jinnai, H.; Hashimoto, T. *Macromolecules* **1999**, *32*, 2585–2596.
(37) Jeon, H. G.; Hudson, S. D.; Ishida, H.; Smith, S. D. *Macromolecules* **1999**, *32*, 1803–1808.
(38) Sijbesma, R. P.; Beijer, F. H.; Brunsveld, L.; Folmer, B. J. B.; Hirschberg, J. H. K. K.; Lange, R. F. M.; Lowe, J. K. L.; Meijer, E. W. *Science* **1997**, *278*, 1601–1604.
(39) Brunsveld, L.; Folmer, B. J. B.; Meijer, E. W.; Sijbesma, R. P. *Chem. Rev.* **2001**, *101*, 4071–4097.
(40) Ikkala, O.; ten Brinke, G. *Science* **2002**, *295*, 2407–2409.
(41) Ikkala, O.; ten Brinke, G. *Chem. Commun.* **2004**, 2131–2137.
(42) Matsushita, Y. *Macromolecules* **2007**, *40*, 771–776.
(43) Hoogenboom, R.; Fournier, D.; Schubert, U. S. *Chem. Commun.* **2008**, *155*, 155–162.
(44) Kosonen, H.; Valkama, S.; Hartikainen, J.; Eerikainen, H.; Torkkeli, M.; Jokela, K.; Serimaa, R.; Sundholm, F.; ten Brinke, G.; Ikkala, O. *Macromolecules* **2002**, *35*, 10149–10154.
(45) Ruokolainen, J.; Makinen, R.; Torkkeli, M.; Makela, T.; Serimaa, R.; ten Brinke, G.; Ikkala, O. *Science* **1998**, *280*, 557–560.
(46) Tucker, P. S.; Paul, D. R. *Macromolecules* **1988**, *21*, 2801–2807.
(47) Jiang, M.; Huang, E.; Xie, J. *Macromol. Chem. Phys.* **1995**, 803–813.
(48) Pan, J.; Chen, M.; Warner, W.; He, M.; Dalton, L.; Hogen-Esch, T. E. *Macromolecules* **2000**, *33*, 7835–7841.
(49) Asari, T.; Arai, S.; Takano, A.; Matsushita, Y. *Macromolecules* **2006**, *39*, 2232–2237.
(50) Segalman, R. A. *Mater. Sci. Eng., R* **2005**, *R48*, 191–226.
(51) Cheng, J. Y.; Ross, C. A.; Smith, H. I.; Thomas, E. L. *Adv. Mater.* **2006**, *18*, 2505–2521.
(52) Segalman, R. A.; Hexemer, A.; Kramer, E. J. *Phys. Rev. Lett.* **2003**, *91*, 196101.
(53) Segalman, R. A.; Hexemer, A.; Kramer, E. J. *Macromolecules* **2003**, *36*, 6831–6839.
(54) Segalman, R. A.; Schaefer, K. E.; Fredrickson, G. H.; Kramer, E. J.; Magonov, S. *Macromolecules* **2003**, *36*, 4498–4506.
(55) Segalman, R. A.; Hexemer, A.; Hayward, R. C.; Kramer, E. J. *Macromolecules* **2003**, *36*, 3272–3288.
(56) Stein, G. E.; Kramer, E. J.; Li, X.; Wang, J. *Phys. Rev. Lett.* **2007**, *98*, 086101.
(57) Stein, G. E.; Kramer, E. J.; Li, X.; Wang, J. *Macromolecules* **2007**, *40*, 2453–2460.
(58) Stein, G. E.; Kramer, E. J.; Li, X.; Wang, J. *Phys. Rev. Lett.* **2007**, *98*, 086101.
(59) Yokoyama, H.; Mates, T. E.; Kramer, E. J. *Macromolecules* **2000**, *33*, 1888–1898.
(60) Park, M.; Harrison, C.; Chaikin, P. M.; Register, R. A.; Adamson, D. H. *Science* **1997**, *276*, 1401–1404.
(61) Tang, C.; Tracz, A.; Kruk, M.; Zhang, R.; Smilgies, D.-M.; Matyjaszewski, K.; Kowalewski, T. *J. Am. Chem. Soc.* **2005**, *127*, 6918–6919.
(62) Morkved, T. L.; Lu, M.; Urbas, A. M.; Ehrichs, E. E.; Jaeger, H. M.; Mansky, P.; Russell, T. P. *Science* **1996**, *273*, 931–933.
(63) Segalman, R. A.; Yokoyama, H.; Kramer, E. *J. Adv. Mater.* **2001**, *13*, 1152–1155.
(64) Cheng, J. Y.; Ross, C. A.; Thomas, E. L.; Smith, H. I.; Vancso, G. J. *App. Phys. Lett.* **2002**, *81*, 3657–3659.
(65) Albalak, R. J.; Thomas, E. L. *J. Polym. Sci., Polym. Phys.* **1994**, *32*, 341–350.
(66) Ryu, D. Y.; Shin, K.; Drockenmuller, E.; Hawker, C. J.; Russell, T. P. *Science* **2005**, *308*, 236–239.
(67) Mansky, P.; Liu, Y.; Huang, E.; Russell, T. P.; Hawker, C. J. *Science* **1997**, *275*, 1458–1460.
(68) Kim, S. O.; Solak, H. H.; Stoykovich, M. P.; Ferrier, N. J.; de Pablo, J. J.; Nealey, P. F. *Nature* **2003**, *424*, 411–414.
(69) Kimura, M.; Misner, M. J.; Xu, T.; Kim, S. H.; Russell, T. P. *Langmuir* **2003**, *19*, 9910–9913.
(70) De Rosa, C.; Park, C.; Thomas, E. L.; Lotz, B. *Nature* **2000**, *405*, 433–437.
(71) Angelescu, D. E.; Waller, J. H.; Register, R. A.; Chaikin, P. M. *Adv. Mater.* **2004**, *16*, 1736–1740.
(72) Ruiz, R.; Kang, H.; Detcheverry, F. A.; Dobisz, E.; Kercher, D. S.; Albrecher, T. R.; de Pable, J. J.; Nealey, P. F. *Science* **2008**, *321*, 936–939.
(73) Bita, I.; Yang, J. K. W.; Ross, C. A.; Thomas, E. L.; Berggren, K. K. *Science* **2008**, *321*, 939–943.
(74) Park, S.; Lee, D. H.; Xu, J.; Kim, B.; Hong, S. W.; Jeong, U.; Xu, T.; Russell, T. P. *Science* **2009**, *323*, 1030–1033.
(75) Tang, C.; Lennon, E. M.; Fredrickson, G. H.; Kramer, E. J.; Hawker, C. J. *Science* **2008**, *322*, 429–432.
(76) Tang, C.; Sivanandan, K.; Stahl, B. C.; Fredrickson, G. H.; Kramer, E. J.; Hawker, C. J. *ACS Nano* **2010**, *4*, 285–291.
(77) Kim, S. H.; Misner, M. J.; Xu, T.; Kimura, M.; Russell, T. P. *Adv. Mater.* **2004**, *16*, 226–231.
(78) Kim, S. H.; Misner, M. J.; Russell, T. P. *Adv. Mater.* **2004**, *16*, 2119–2123.
(79) Bang, J.; Kim, B. J.; Stein, G. E.; Russell, T. P.; Kramer, E. J.; Hawker, C. J. *Macromolecules* **2007**, *40*, 7019–7025.
(80) Park, S. C.; Kim, B. J.; Hawker, C. J.; Kramer, E. J.; Bang, J.; Ha, J. S. *Macromolecules* **2007**, *40*, 8119–8124.
(81) Chiefari, J.; Chong, Y. K.; Ercole, F.; Krstina, J.; Jeffery, J.; Le, T. P.; Mayadunne, R. T. A.; Meijs, G. F.; Moad, C. L.; Moad, G.; Rizzardo, E.; Thang, S. H. *Macromolecules* **1998**, *31*, 5559–5562.
(82) Hawker, C. J.; Bosman, A. W.; Harth, E. *Chem. Rev.* **2001**, *101*, 3661–3688.
(83) Kamigaito, M.; Ando, T.; Sawamoto, M. *Chem. Rev.* **2001**, *101*, 3689–3745.
(84) Matyjaszewski, K.; Xia, J. H. *Chem. Rev.* **2001**, *101*, 2921–2990.
(85) *Polymer Handbook*; Brandrup, J., Immergut, E. H., Gurulke, E. A., Abe, A., Bloch, D. R., Eds.; Wiley: New York, 1999.
(86) Yurt, S.; Anyanwu, U. K.; Scheintaub, J. R.; Coughlin, E. B.; Venkataraman, D. *Macromolecules* **2006**, *39*, 1670–1672.
(87) Zhang, M.; Yang, L.; Yurt, S.; Misner, M. J.; Chen, J. T.; Coughlin, E. B.; Venkataraman, D.; Russell, T. P. *Adv. Mater.* **2007**, *19*, 1571–1576.
(88) Fredrickson, G. H.; Ganesan, V.; Drolet, F. *Macromolecules* **2002**, *35*, 16–39.
(89) Fredrickson, G. H. *The Equilibrium Theory of Inhomogeneous Polymers*; Clarendon Press: Oxford, U.K., 2006.
(90) Coleman, M. W.; Graf, J. F.; Painter, P. C. *Specific Interactions and the Miscibility of Polymer Blends*; Technomic Pub. Co.: Lancaster, PA, 1991.